

Supplementary material

Efficient conversion of montmorillonite-derived porous nano-silica to nano-silicon for lithium-ion batteries anode

Jing Du^{a,b,c}, Jieyang Xie^{a,b,c}, Shoushu Wei^{a,b,c}, Tao Xiong^{a,b,c}, Shiya He^{a,b,c}, Haiming

Huang^{a,b,c}, Qingze Chen^{a,b,c*}, Runliang Zhu^{a,b,c}, Jianxi Zhu^{a,b,c}

^a *CAS Key Laboratory of Mineralogy and Metallogeny, Guangdong Provincial Key Laboratory of Mineral Physics and Materials, Guangzhou Institute of Geochemistry, Chinese Academy of Sciences, Guangzhou, 510640, China*

^b *CAS Center for Excellence in Deep Earth Science, Guangzhou, 510640, China*

^c *University of Chinese Academy of Sciences, Beijing, 100049, China*

* Corresponding author

Fax: 86-020-85297082

Phone: 86-020-85297082

E-mail: chenqingze@gig.ac.cn

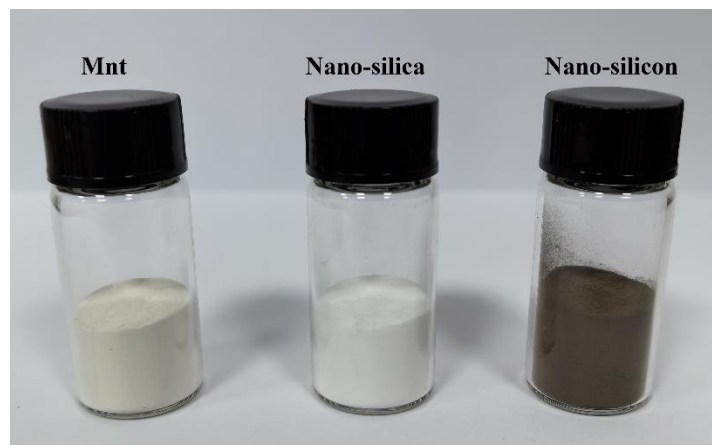


Figure S1. The photographic images of Mnt, nano-silica, and nano-silicon.

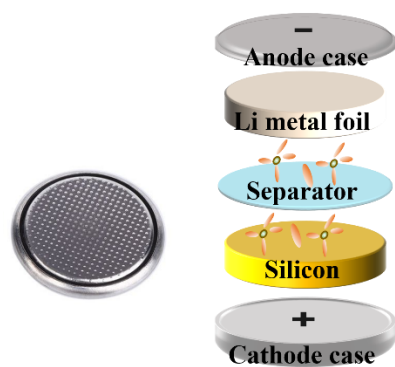


Figure S2. Photographic image of the coin-type half-cell and the corresponding schematic diagram of its structural composition.

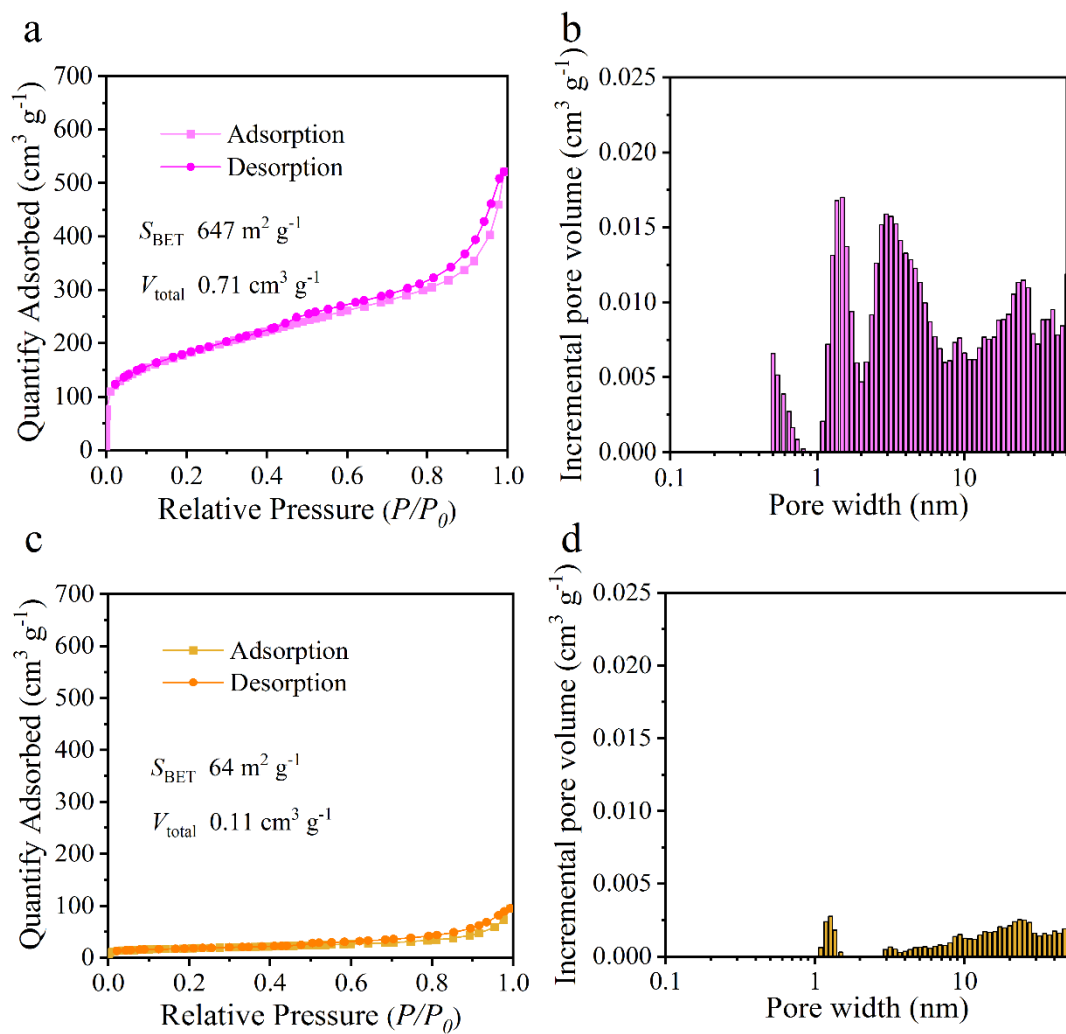


Figure S3. The N_2 adsorption/desorption isotherms and pore size distribution of n- SiO_2 (a, b) and Mnt (c,d).

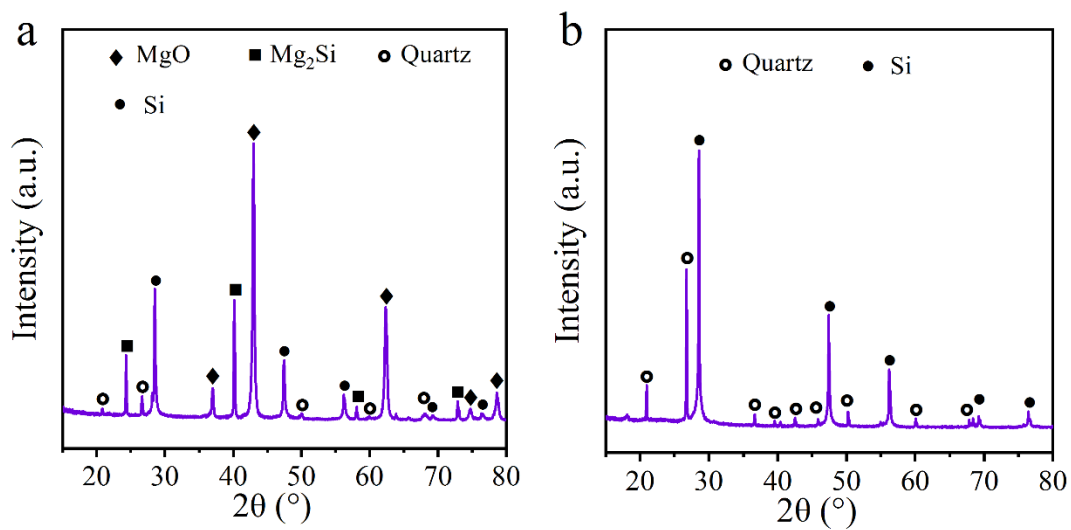


Figure S4. The XRD patterns of (a) the intermediate products after the magnesiothermic reduction of quartz powder (the NaCl was removed by water), and (b) the final products after HCl leaching.

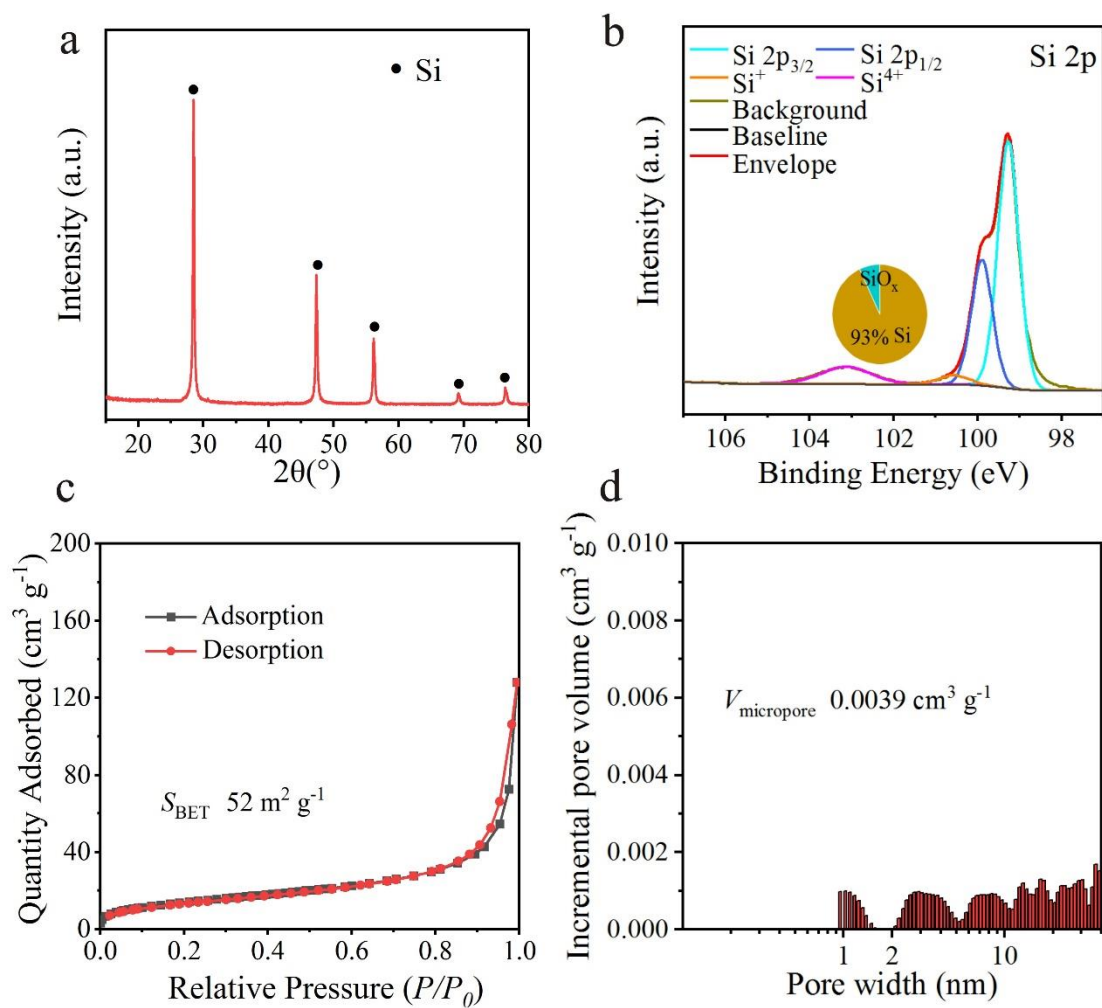


Figure S5. The XRD pattern (a), Si 2p XPS spectrum (b), N₂ adsorption/desorption isotherms (c), and pore size distribution of SiSiO₂-HF (d) of SiSiO₂-HF.

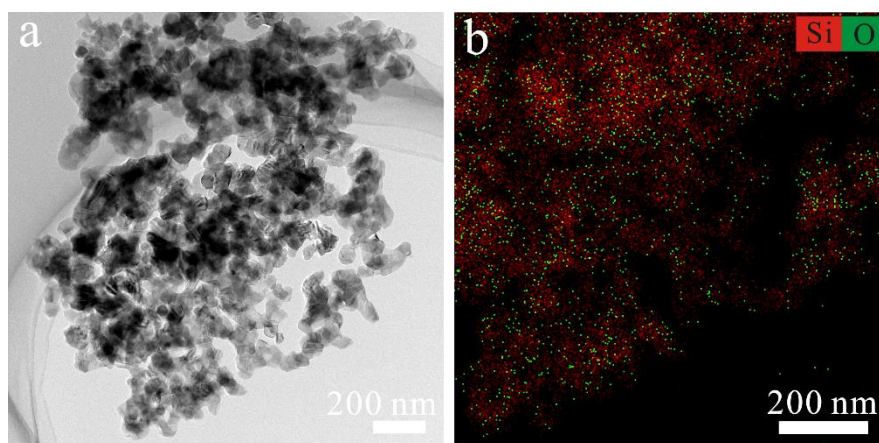


Figure S6. TEM image (a) and corresponding EDS mapping (b) of $\text{SiSiO}_2\text{-HF}$.

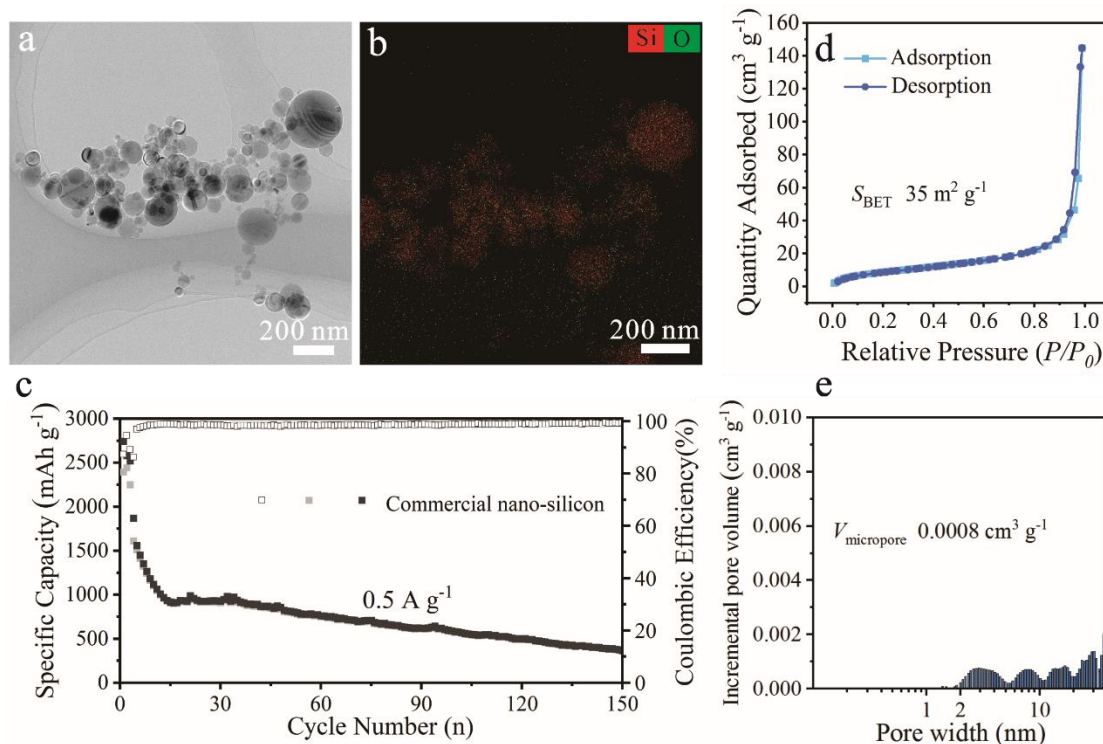


Figure S7. (a) TEM image, (b) EDS mapping, (c) cycling performance at a current density of 0.5 A g^{-1} (0.1 A g^{-1} for the initial three cycles), (d) N_2 adsorption/desorption isotherms, and (e) pore size distribution of commercial nano-silicon.

The commercial nano-silicon material was prepared by plasma-assisted chemical vapor deposition. The TEM image of the commercial nano-silicon revealed a spherical structure with diameters ranging from 10 to 200 nm, while EDS analysis indicated an oxygen content of $\sim 3 \text{ wt.}\%$. The specific surface area and total pore volume of commercial nano-silicon were $35 \text{ m}^2 \text{ g}^{-1}$ and $0.101 \text{ cm}^3 \text{ g}^{-1}$, respectively.

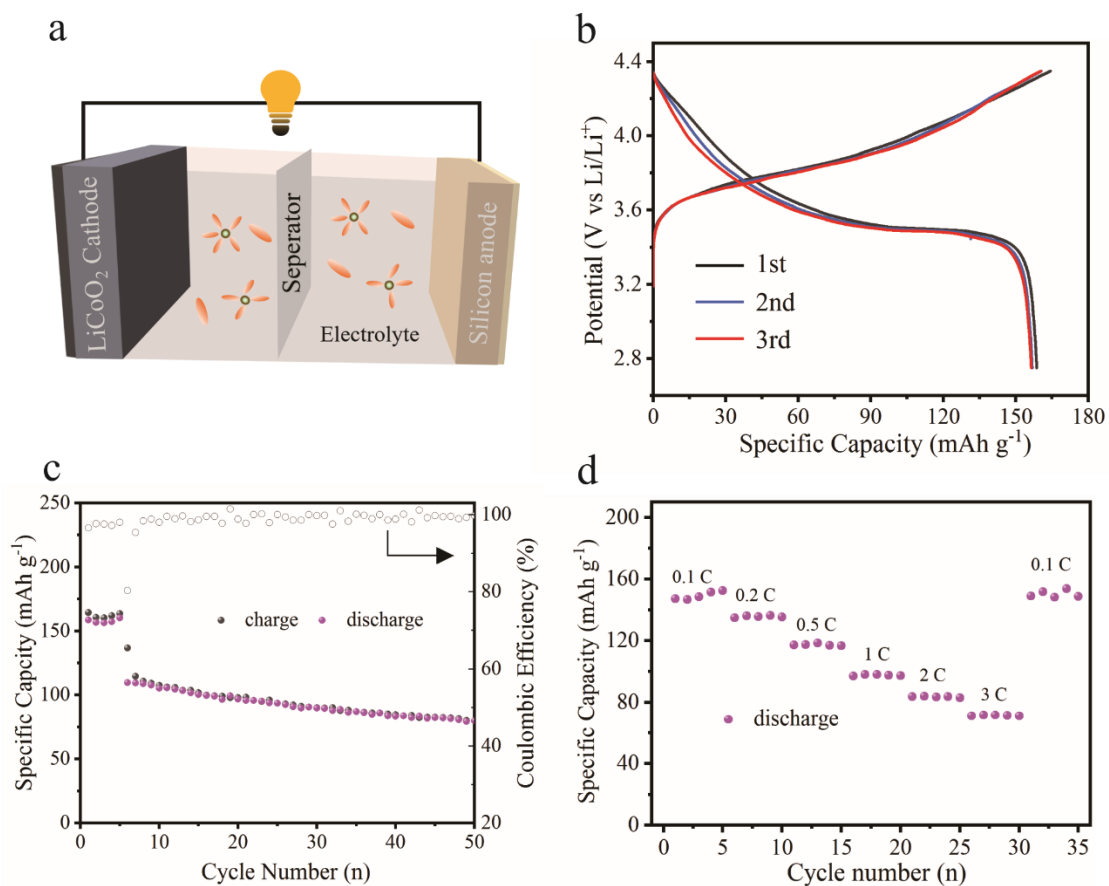


Figure S8. (a) Schematic of full-cell configuration for Li-ion battery with a silicon anode and LCO cathode; (b) the galvanostatic charge-discharge curves of the Si//LCO full cell for initial three cycles at 0.05 C; (c) Cycling performance of Si//LCO full cell at 0.5 C (0.05 C for initial five cycles); (d) Rate performance of Si//LCO full cell at various current densities.

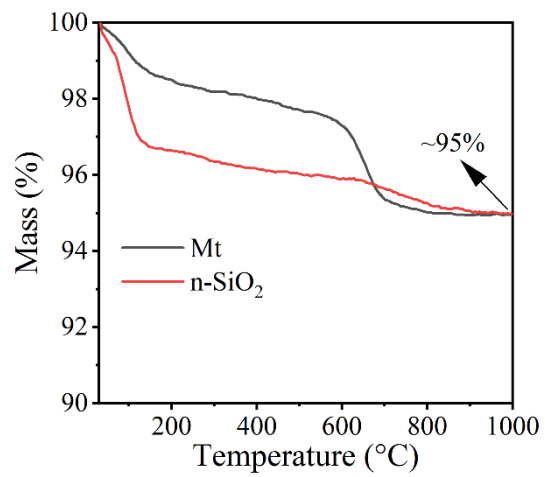


Figure S9. TG curves of n-SiO₂ and Mt.

Table S1. Chemical composition of Mnt and n-SiO₂ (wt%).

Samples	SiO ₂	Al ₂ O ₃	TFe ₂ O ₃ *	MgO	CaO	TiO ₂	ZrO ₂	K ₂ O	Na ₂ O
Mnt	64.95	15.37	9.16	5.14	4.28	0.50	0.39	0.17	0.04
n-SiO ₂	99.09	0.45	<0.01	<0.01	0.10	0.10	0.01	0.08	0.16

TFe₂O₃* represents the total iron content in the sample, expressed as iron(III) oxide (Fe₂O₃).

Table S2. Si 2p XPS results of Med-Si_{Mnt}, Med-Si_{SiO₂}, Si_{Mnt}, and Si_{SiO₂}.

Atomic (%)	Si 2p _{3/2}	Si 2p _{1/2}	Si ⁺	Si ²⁺	Si ⁴⁺
Med-Si _{Mnt}	29.53	29.54	/	/	40.93
Med-Si _{SiO₂}	43.94	43.95	/	/	12.11
Si _{Mnt}	33.26	33.27	1.81	0.66	31.01
Si _{SiO₂}	42.44	42.46	1.21	0.43	13.46

Table S3. The conversion rate of silica to silicon for Mnt, n-SiO₂, and quartz powder through magnesiothermic reduction.

Sample	Mass ratio of Elements		Conversion rate of silica to silicon
	Si	O	
Si _{Mnt}	89%	11%	79%
Si _{SiO₂}	95%	5%	91%
Si _{Qz}	80%	20%	62%

The O element in the product was assumed to be exclusively in the form of silica. The conversion rate of nano-silicon from silica was assessed using the following formula:

$$R = \left(1 - \frac{Mo * 60}{32}\right) \times 100\%$$

R represents the conversion rate of silica to silicon; *Mo* represents the mass of the O element in the product.

Table S4. The yield of Si_{Mnt} and Si_{SiO_2} based on 1 g precursor.

Sample	Theoretical product weight (mg)	Actual product weight (mg)	Yield (%)
Si_{Mnt}	288	310	110
Si_{SiO_2}	439	406	92

The theoretical product weight was based on data in Table S1. To accurately determine the theoretical weight of silicon in the product, the water content in Mnt and n-SiO₂ was excluded. The water content in Mnt and n-SiO₂ are both 5 wt% as determined by thermogravimetric data (**Figure S9**).